IEEE Photonics Journal
An IEEE Photonics Society Publication

Open Access

Improved Performance of ITO-Free Organic Solar Cells Using a Low-Workfunction and Periodically Corrugated Metallic Cathode

Volume 4, Number 5, October 2012

Yu Jin
Jing Feng
Yan-Hui Wang
Ming Xu
Tian Lan
Yan-Gang Bi
Qi-Dai Chen
Hai-Yu Wang
Hong-Bo Sun, Member, IEEE

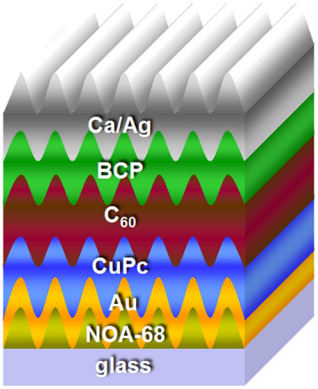

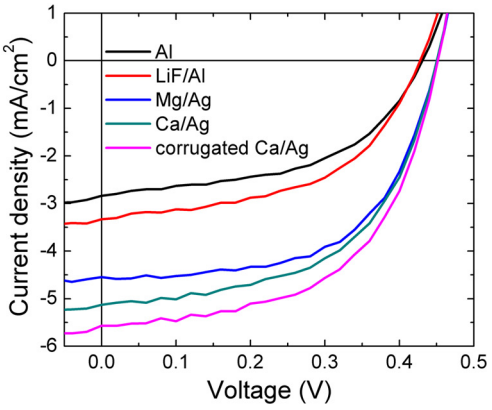

DOI: 10.1109/JPHOT.2012.2212423
1943-0655/$31.00 ©2012 IEEE

IEEE photonics SOCIETY

IEEE

Improved Performance of ITO-Free Organic Solar Cells Using a Low-Workfunction and Periodically Corrugated Metallic Cathode

Yu Jin,[1] Jing Feng,[1] Yan-Hui Wang,[1] Ming Xu,[1] Tian Lan,[1] Yan-Gang Bi,[1] Qi-Dai Chen,[1] Hai-Yu Wang,[1] and Hong-Bo Sun,[1,2] *Member, IEEE*

[1]State Key Laboratory on Integrated Optoelectronics, College of Electronic Science and Engineering, Jilin University, Changchun 130012, China
[2]College of Physics, Jilin University, Changchun 130023, China

DOI: 10.1109/JPHOT.2012.2212423

Manuscript received July 10, 2012; revised July 31, 2012; accepted August 3, 2012. Date of publication August 23, 2012; date of current version September 5, 2012. This work was supported by the National Science Foundation of China (NSFC) under Grants 61177024, 60977025, and 61107024. Corresponding authors: J. Feng and H. B. Sun (e-mail: jingfeng@jlu.edu.cn; hbsun@ieee.org).

Abstract: The indium–tin-oxide-free organic solar cells (OSCs) have been fabricated using a semitransparent Au film as anode. A comparative study between the OSCs with different metal cathodes shows that formation of an ideal ohmic contact at low-workfunction Ca and the organic interface reduces series resistance and increases the carrier collection. Moreover, a periodic corrugation was introduced into the device structure, which leads to an enhanced light absorption in the OSCs by elongating the optical path of the incident light inside the absorber material. The highest power conversion efficiency of an optimal OSC with a Au anode and a corrugated Ca/Ag cathode is 1.4%, which is significantly improved in contrast to 0.61% for the OSC with a planar Al cathode.

Index Terms: Organic solar cells (OSCs), low-workfunction metal, periodic corrugation, Au anode.

1. Introduction

Organic solar cells (OSCs) are potential candidates for the next generation of photovoltaic devices because of their advantages over their inorganic counterparts: they are low-cost, flexible, and appropriate for large-scale applications [1]–[4]. Indium–tin oxide (ITO) is the most commonly used transparent electrode material in OSCs because it provides a combination of transparency and conductivity. However, a global shortage of indium, more than 80% of the fabrication cost [5], and poor compatibility with flexible substrates have limited its commercial applications. A roll-to-roll process is compatible to ITO-free OSCs on the flexible substrates [6]–[9]. Transparent flexible conductive materials such as conducting polymers [10]–[12], carbon nanotube films [13]–[15], graphene [16], random networks of metallic nanowires and nanometallic/micrometallic grids [17], [18] have been shown to be promising alternatives to ITO. Unfortunately, very few of these electrodes have yielded OSCs with performances comparable to those utilizing ITO.

Recently, Au has attracted attention as an electrode material to replace ITO in OSCs [19]–[22] because of its high workfunction, high conductivity, simple fabrication process, and compatibility with flexible materials [23]. Moreover, Au is more easily extracted from the earth crust and can also be applied very thin, so that a short energy payback time is expected [24]. In this paper, a semitransparent Au film instead of the ITO is used as the anode in the OSCs. The performance of

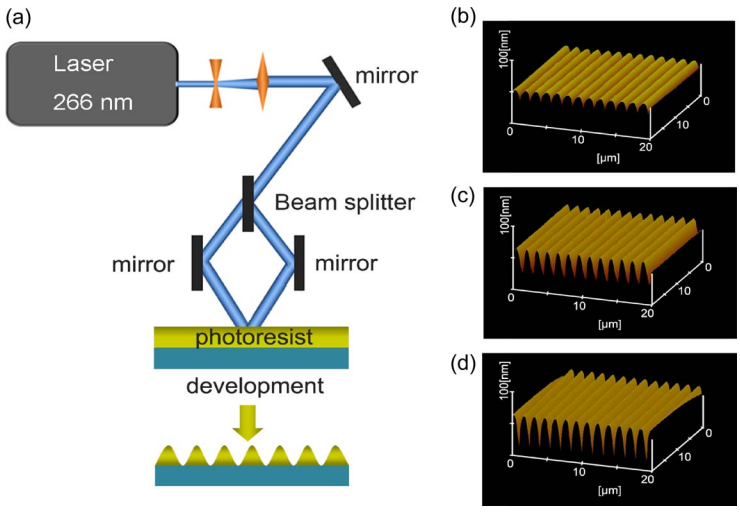

Fig. 1. (a) Scheme diagram of the process steps for fabrication of micrometer-periodical corrugation by holographic lithography and AFM images of surface morphology of periodic corrugation with (b) 20-nm, (c) 35-nm, and (d) 45-nm groove depth, respectively.

the Au-based OSCs has been improved using an ultrathin low-workfunction metal Ca modified thick Ag as cathode and introducing the periodic corrugation into the device. We demonstrated that an ideal ohmic contact at the Ca/organic interface increases the carrier harvest and reduces the series resistance of the OSCs. Moreover, light trapping and more efficient capture and separation of excitons at the interface between the donor and the acceptor induced by the introduction of the periodic corrugation have played an important role in improving short-circuit current. As a result, the power conversion efficiency (PCE) of optimally corrugated OSCs is significantly improved.

2. Experimental Details

2.1. Preparation of Periodically Corrugated Substrate

A two-beam laser interference microfabrication system was set up, as shown in Fig. 1(a). A continuous laser with a wavelength of 266 nm (MBD E-200, Coherent Inc., USA) was used as the light source. Before the fabrication of the cells, the glass substrates were precleaned sequentially by acetone, ethanol, and deionized water in an ultrasonic bath for 10 min and finally dried in a N_2 stream. A 120-nm-thick layer of photoresist (NOA-68, Norland Inc., USA) was spin-coated onto the cleaned glass substrates and exposed by two beams, which were split from the UV laser and had a beam diameter of $\sim$6 mm. After the exposure, the samples were baked for 1 min at 95 °C on a hotplate and then developed in acetone. By controlling the writing angle and exposure time, 1-D corrugations with a period of 1.5 μm and groove depths of 20, 35, and 45 nm were achieved. The morphologies of the microstructures were characterized by atomic force microscopy (AFM, Digital Instruments Nanoscope IIIA, Veeco Inc., USA) in tapping mode, and the AFM images of the 20-, 35-, and 45-nm grooves are shown in Fig. (b)–(d), respectively.

2.2. Fabrication and Characterization of OSCs

The OSCs were fabricated on both glass substrates coated with the corrugated photoresist and bare glass substrates. Then, the substrates were immediately loaded into a thermal evaporation chamber. A 20-nm-thick Au layer ($\sim$10 Ω/sq) was deposited onto the substrates by thermal evaporation through a shadow mask. An electron donor layer of copper phthalocyanine (CuPc, 35 nm), an electron acceptor layer of fullerene (C_{60}, 70 nm), and an exciton-blocking layer of bathocuproine (BCP, 10 nm) were evaporated sequentially. As shown in Fig. 2(a), devices A, B, C, and D were

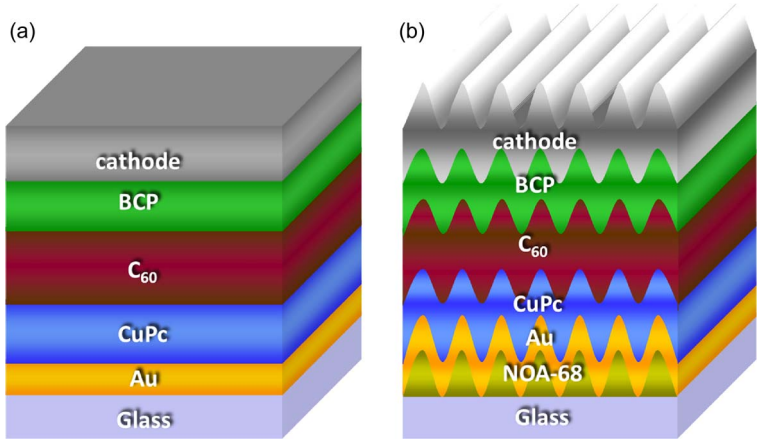

Fig. 2. Schematic structures of OSC devices with (a) and without (b) micrometer-periodical corrugation.

fabricated on a bare substrate with Al (80 nm), LiF/Al (1 nm/80 nm), Mg/Ag (3 nm/80 nm), and Ca/Ag (3 nm/80 nm) cathodes, respectively. Devices E, F, and G were fabricated on corrugated substrates with 20-, 35-, and 45-nm groove depths, respectively, so that the periodic corrugations were formed throughout the device structure, as shown in Fig. 2(b). The cathode of all the corrugated devices is Ca/Ag. All organic and metallic films were thermally evaporated under high vacuum $(5 \times 10^{-4}$ Pa). All organic materials were purchased from LumTec. Corp. and used as received. The active area of the device is 2×2 mm^2. The thickness of each layer was monitored by quartz crystals and calibrated by a spectroscopic ellipsometer (J. A. Woollam Co., Inc., USA). The current density–voltage (J–V) curves of the OSCs were measured by a Keithley 2400 sourcemeter under 1 sun (100 mW/cm^2) simulated AM 1.5-G illumination. The reflectance spectra of the samples were measured by a UV-vis spectrophotometer (UV-2550, SHIMADZU Co., Inc., Japan). All values herein are given without mismatch correction.

3. Results and Discussion

3.1. Optimization of the Cathode Structure

First, the Au-based OSCs using Al (A), LiF/Al (B), Mg/Ag (C), and Ca/Ag (D) cathodes were fabricated and characterized to obtain an optimized cathode structure. The workfunction of Al, Mg, and Ca is 4.28, 3.6, and 2.9 eV, respectively. The J–V characteristics of the prepared OSCs are shown in Fig. 3. The detailed results are given in Table 1. The interface between the electrode and the organic active layer plays an important role in the carrier collection and interfacial resistance [25]–[27]. From the J–V curves, it can be seen that the short-circuit current (J_{sc}) of the OSCs is strongly dependent on the workfunction of the cathode. The OSC with Al cathode (A) shows poor photovoltaic behavior $(V_{oc} = 0.42$ V, $J_{sc} = 2.83$ mA/cm^2, PCE $= 0.61\%)$. When Al was modified by LiF, slightly higher J_{sc} (3.33 mA/cm^2) and PCE (0.74%) were obtained. Mg and Ca with a further lower workfunction of 3.6 and 2.9 eV, respectively, were used in devices C and D. As a result, the highest V_{oc} (0.46 V), photocurrent (5.12 mA/cm^2), and PCE (1.27%) were observed for device D using Ca/Ag as cathode. The PCE is increased by 1 time over the PCE of device A with Al cathode.

The major contributing factor to the obvious increment is the formation of an ideal ohmic contact at the organic/cathode interface due to the very good matching of the Fermi levels of Ca (2.9 eV) to the lowest unoccupied molecular orbital of the BCP (2.9–3.0 eV) [28], [29], which reduce the series resistance and enhance the carrier harvest. On the other hand, a large workfunction difference between the anode of Au (5.1 eV) and the electrode of Ca (2.9 eV) forms a strong built-in electric field in active layers, which promotes the separation of excitons and reduces the recombination of carriers. In both cases, a high photovoltaic performance can be achieved.

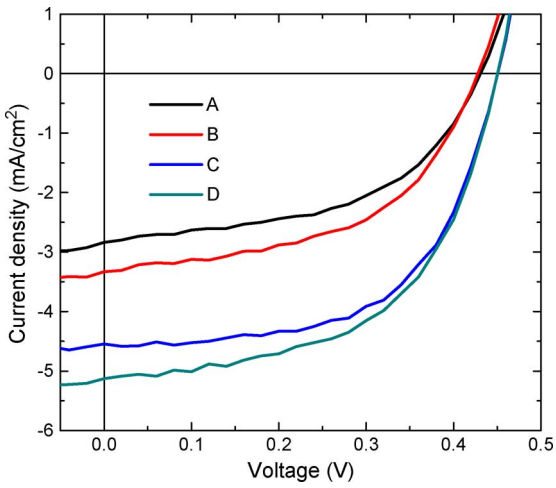

Fig. 3. *J–V* characteristics of the planar OSCs (devices A, B, C, and D) with different metal cathodes (Al, LiF/Al, Mg/Ag, and Ca/Ag).

TABLE 1

Photovoltaic parameters of planar OSCs (devices A, B, C, and D) with different metal cathodes (Al, LiF/Al, Mg/Ag, and Ca/Ag)

Cell device	Voc (V)	Jsc (mA /cm^2)	FF %	PCE %
Cell device A	0.42	2.83	51	0.61
Cell device B	0.44	3.33	52	0.74
Cell device C	0.46	4.51	57	1.21
Cell device D	0.46	5.13	55	1.27

3.2. Performance of the OSCs with Corrugated Structure

The corrugations with various groove depths were introduced into the planar device with the optimal Ca/Ag cathode to further improve its properties. The *J–V* characteristics of these OSCs (devices E, F, and G) are shown in Fig. 4, and the detail performance is summarized in Table 2. Comparing with the planar device with the same cathode (device D), the photocurrent of corrugated OSCs increases with increasing groove depth. The J_{sc} of corrugated device G with a 45-nm groove depth is 5.57 mA/cm^2, which is higher than that of planar device D (5.12 mA/cm^2). The PCE increases from 1.27% for planar devices to 1.4% for device G with a groove depth of 45 nm, corresponding to an enhancement of 10%.

To verify that this efficiency enhancement is induced by the corrugation, the absorption spectra of the corrugated devices with various groove depths were compared with that of the planar device, as shown in Fig. 5. The light is incident through the semitransparent Au anode, and the reflection spectra have been measured. Absorption spectra are obtained from the complementary relation between reflection and absorption. The peaks at 645 and 710 nm correspond to the intrinsic absorption of CuPc, while the peak at 550 nm is due to the resonance of the microcavity formed by the two metallic electrodes. The absorption significantly increases with the groove depth in the short-wavelength region (less than 500 nm) and also in the absorption region of CuPc, which indicates that more light is trapped in the OSCs with the corrugated structure. The increased trapping of light results in the grating depth-dependent enhancement of light absorption and J_{sc}.

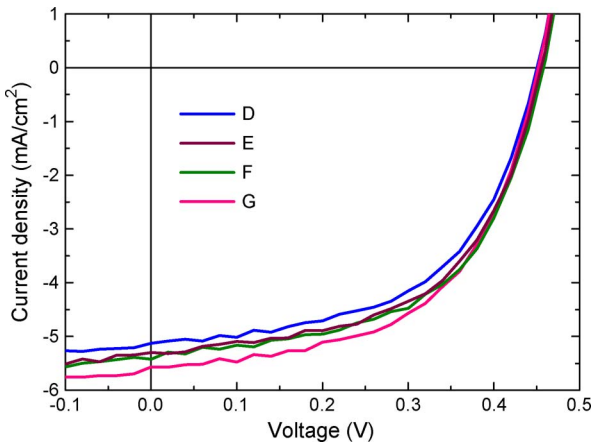

Fig. 4. *J–V* characteristics of planar device D and corrugated devices E, F, and G with different groove depths.

TABLE 2

Photovoltaic parameters of planar device D and corrugated devices E, F, and G with different groove depths

Cell device	Voc (V)	Jsc (mA /cm^2)	FF %	PCE %	Height (nm)
Cell device D	0.46	5.13	55	1.27	
Cell device E	0.46	5.30	55	1.34	20
Cell device F	0.46	5.42	55	1.37	35
Cell device G	0.46	5.57	55	1.40	45

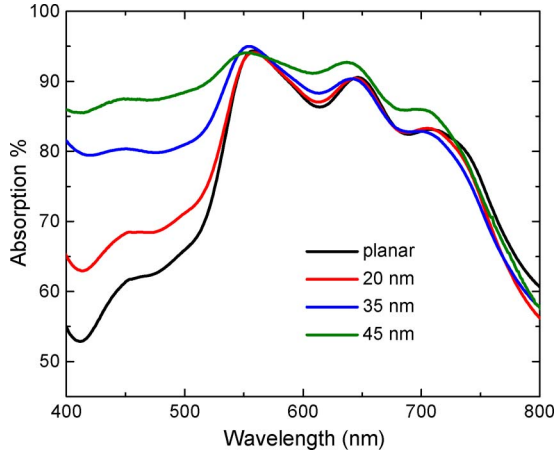

Fig. 5. Absorption spectra of the planar and corrugated devices with 20-, 35-, and 45-nm groove depths.

The period of 1.5 μm is much larger than the wavelength scale; therefore, the effect of surface plasmons promoting better absorption can be ruled out. The elongated optical path of the incident light inside the absorber material due to the structured metal electrode surfaces is the most probable mechanism for the absorption enhancement [30]. The light reflected by the microstructured

back cathode is no longer normal to the substrate plane; thus, it crosses the absorber layer at a greater angle on the way back. Therefore, the path for absorption is elongated, and light is concentrated in the absorber. In addition, the larger junction interface area induced by the corrugation may also contribute to the increased efficiency [31]–[33] because the number of excitons generated in CuPc within a diffusion length of the junction interface increases proportionately to the junction area.

4. Conclusion

In summary, the performance of OSCs with Au anode has been improved by employing a low-workfunction and periodically corrugated Ca/Ag cathode. The experimental results show that the performance of planar devices is dependent on the workfunction of the cathode. The PCE of the planar OSC with an optimal Ca/Ag cathode exhibits 2 times enhancement compared with that of the device with Al cathode. Moreover, the performance of Au-based OSCs has been further improved by employing corrugated structures. The corrugated metal electrode surfaces can increase the length of the optical path of the incident light inside the absorber material and enhance light trapping. The increased junction interface area induced by the corrugation also contributed to the increased efficiency by improving the capture of the excitons at the corrugated interface. As a result, the PCE exhibits a further increment of 10% comparing with that of the planar device.

References

[1] N. S. Sariciftci, L. Smilowitz, A. J. Heeger, and F. Wudl, "Photoinduced electron transfer from a conducting polymer to buckminsterfullerene," *Science*, vol. 258, no. 27, pp. 1474–1476, Nov. 1992.

[2] P. Peumans, A. Yakimov, and S. R. Forrest, "Small molecular weight organic thin-film photodetectors and solar cells," *J. Appl. Phys.*, vol. 93, no. 7, pp. 3693–3723, Jul. 2003.

[3] F. C. Krebs, "Fabrication and processing of polymer solar cells: A review of printing and coating techniques," *Sol. Energy Mater. Sol. Cells*, vol. 93, no. 4, pp. 394–412, Apr. 2009.

[4] C. W. Tang, "Two layer organic photovoltaic cell," *Appl. Phys. Lett.*, vol. 48, no. 2, pp. 183–185, Jan. 1986.

[5] N. Espinosa, R. G. Valverde, A. Urbina, and F. C. Krebs, "A life cycle analysis of polymer solar cell modules prepared using roll-to-roll methods under ambient conditions," *Sol. Energy Mater. Sol. Cells*, vol. 95, no. 5, pp. 1293–1302, May 2011.

[6] R. Sndergaard, M. Hösel, D. Angmo, T. T. Larsen-Olsen, and F. C. Krebs, "Roll-to-roll fabrication of polymer solar cells," *Mater. today*, vol. 15, no. 1/2, pp. 36–49, Jan./Feb. 2012.

[7] M. Manceau, D. Angmo, M. Jrgensen, and F. C. Krebs, "ITO-free flexible polymer solar cells: From small model devices to roll-to-roll processed large modules," *Org. Electron.*, vol. 12, no. 9, pp. 568–574, Dec. 2011.

[8] F. C. Krebs, "All solution roll-to-roll processed polymer solar cells free from indium–tin-oxide and vacuum coating steps," vol. 10, no. 5, pp. 761–768, Aug. 2009.

[9] F. C. Krebs, "Roll-to-roll fabrication of monolithic large-area polymer solar cells free from indium–tin-oxide," *Sol. Energy Mater. Sol. Cells*, vol. 93, no. 9, pp. 1636–1641, Sep. 2009.

[10] Y. H. Zhou, F. L. Zhang, K. Tvingstedt, S. Barrau, F. H. Li, W. J. Tian, and O. Lnganäs, "Investigation on polymer anode design for flexible polymer solar cells," *Appl. Phys. Lett.*, vol. 92, no. 23, p. 23308, Jun. 2008.

[11] S. K. Hau, H. L. Yip, J. Y. Zhou, and A. K. Y. Jen, "Indium tin oxide-free semi-transparent inverted polymer solar cells using conducting polymer as both bottom and top electrodes," *Org. Electron.*, vol. 10, no. 7, pp. 1401–1407, Nov. 2009.

[12] S. I. Na, S. S. Kim, J. Jo, and D. Y. Kim, "Efficient and flexible ITO-free organic solar cells using highly conductive polymer anodes," *Adv. Mater.*, vol. 20, no. 21, pp. 4016–4067, Nov. 2008.

[13] S. Tanaka, K. Mielczarek, R. Ovalle-Robles, B. Wang, D. Hsu, and A. A. Zakhidov, "Monolithic parallel tandem organic photovoltaic cell with transparent carbon nanotube interlayer," *Appl. Phys. Lett.*, vol. 94, no. 11, p. 113506, Mar. 2009.

[14] M. H. Liang, B. Luo, and L. J. Zhi, "Application of graphene and graphene-based materials in clean energy-related devices," *Int. J. Energy Res.*, vol. 33, no. 13, pp. 1161–1170, Oct. 2009.

[15] T. M. Bames, J. D. Bergeson, R. C. Tenent, B. A. Larsen, G. Teeter, K. M. Jones, J. L. Blachburn, and J. V. D. Lagemaat, "Carbon nanotube network electrodes enabling efficient organic solar cells without a hole transport layer," *Appl. Phys. Lett.*, vol. 96, no. 24, p. 243 309, Jun. 2010.

[16] X. Wang, L. J. Zhi, N. Tsao, Tomovi, J. Li, and K. Müllen, "Transparent carbon films as electrodes in organic solar cells," *Angew. Chem. Int. Ed.*, vol. 47, no. 16, pp. 2990–2992, Apr. 2008.

[17] J. Y. Lee, S. T. Connor, Y. Cui, and P. Peumans, "Solution-processed metal nanowire mesh transparent electrodes," *Nano Lett.*, vol. 8, no. 2, pp. 689–692, Feb. 2008.

[18] B. P. Rand, P. Peumans, and S. R. Forrest, "Long-range absorption enhancement in organic tandem thin-film solar cells containing silver nanoclusters," *J. Appl. Phys.*, vol. 96, no. 12, pp. 7519–7526, Dec. 2004.

[19] P. Vivo, J. Jukola, M. Ojala, V. Chukharev, and H. Lemmetyinen, "Influence of Alq3–Au cathode on stability and efficiency of a layered organic," *Sol. Energy Mater. Sol. Cells*, vol. 92, no. 11, pp. 1416–1420, Jul. 2008.

[20] C. D. Wang and W. C. H. Choy, "Efficient hole collection by introducing ultra-thin UV–ozone treated Au in polymer solar cells," *Sol. Energy Mater. Sol. Cells*, vol. 95, no. 3, pp. 904–908, Mar. 2011.
[21] H. M. Stec, R. J. Williams, T. S. Jones, and R. A. Hatton, "Ultrathin transparent Au electrodes for organic photovoltaics fabricated using a mixed mono-molecular nucleation layer," *Adv. Funct. Mater.*, vol. 21, no. 9, pp. 1709–1716, May 2011.
[22] S. Zhang, Z. J. Chen, L. X. Xiao, B. Qu, and Q. H. Gong, "Organic solar cells with 2-Thenylmercaptan/Au self-assembly film as buffer layer," *Sol. Energy Mater. Sol. Cells*, vol. 96, no. 2, pp. 917–920, Mar. 2011.
[23] F. Wang, Z. J. Chen, L. X. Xiao, B. Qu, and Q. H. Gong, "Papery solar cells based on dielectric/metal hybrid transparent cathode," *Sol. Energy Mater. Sol. Cells*, vol. 94, no. 7, pp. 1270–1274, Jul. 2010.
[24] N. Espinosa, M. Hösel, D. Angmo, and F. C. Krebs, "Solar cells with one-day energy payback for the factories of the future," *Energy Environ. Sci.*, vol. 5, no. 1, pp. 5117–5132, Jan. 2012.
[25] C. J. Brabec, S. E. Shaheen, C. Winder, N. S. Sariciftci, and P. Denk, "Effect of LiF/metal electrodes on the performance of plastic solar cells," *Appl. Phys. Lett.*, vol. 80, no. 7, pp. 1288–1290, Feb. 2002.
[26] V. D. Mihailetchi, P. W. M. Blom, J. C. Hummelen, and M. T. Rispens, "Cathode dependence of the open-circuit voltage of polymer: Fullerene bulk heterojunction solar cells," *J. Appl. Phys.*, vol. 94, no. 10, pp. 6849–6854, Nov. 2003.
[27] H. L. Yip, S. K. Hau, N. S. Baek, H. Ma, and A. K. Y. Jen, "Polymer solar cells that use self-assembled-monolayer-modified ZnO/metals as cathodes," *Adv. Mater.*, vol. 20, no. 12, pp. 2376–2382, Jun. 2008.
[28] X. M. Wu, L. Y. Shen, Y. L. Hua, M. S. Dong, Y. J. Su, Z. Q. Jiao, X. Y. Yang, and S. G. Yin, "Highly efficient flexible organic light-emitting devices utilizing F4-TCNQ/m-MTDATA multiple quantum well structures," *J. Lumin.*, vol. 132, no. 5, pp. 1261–1264, May 2012.
[29] S. M. Tekarli, T. R. Cundari, and M. A. Omary, "Rational design of macrometallocyclic trinuclear complexes with superior π-acidity and π-basicity," *J. Amer. Chem. Soc.*, vol. 130, no. 5, pp. 1669–1675, Feb. 2008.
[30] L. Müller-Meskamp, Y. H. Kim, T. Roch, H. Hofmann, R. Scholz, S. Eckardt, K. Leo, and A. F. Lasagni, "Efficiency enhancement of organic solar cells by fabricating periodic surface textures using direct laser interference patterning," *Adv. Mater.*, vol. 24, no. 7, pp. 906–910, Feb. 2012.
[31] M. S. Kim, J. S. Kim, J. C. Cho, M. Shtein, L. J. Guo, and J. Kim, "Flexible conjugated polymer photovoltaic cells with controlled heterojunctions fabricated using nanoimprint lithography," *Appl. Phys. Lett.*, vol. 90, no. 12, pp. 123113-1–123113-3, Mar. 2007.
[32] S. I. Na, S. S. Kim, S. S. Kwon, J. Jo, J. Kim, T. Lee, and D. Y. Kim, "Surface relief gratings on poly (3-hexylthiophene) and fullerene blends for efficient organic solar cells," *Appl. Phys. Lett.*, vol. 91, no. 17, pp. 173509-1–173509-3, Oct. 2007.
[33] C. Goh, K. M. Coakley, and M. D. McGehee, "Nanostructuring titania by embossing," *Nano Lett.*, vol. 5, no. 8, pp. 1545–1549, Jun. 2005.